(2011) have recently reported that in the living cortex, CORT exposure leads to the loss of stable, mature spines with increasing filopodial and thin spines and spine turnover rates. The mechanism revealed by our study would serve a molecular basis to explain those events concerning spine remodeling through a perspective of F-actin dynamics.

CORT downregulated the CaD expression levels in hippocampal neurons and suppressed the fibro-type CaD promoter's SRF/CArG-box-dependent activity (Fig. 6). In this regard, activated GR inhibits SRF activity in human prostate adenocarcinoma cells (Yemelyanov et al., 2007). We previously demonstrated that GC upregulates CaD expression via positive GRE-like sequences in both human lung cancer cells and cortical neural progenitor cells (Mayanagi et al., 2008; Fukumoto et al., 2009). However, in hippocampal neurons the GRE-like sequences did not function for the negative regulation of CaD transcription and the direct contribution of GR via the GRE-like sequences, therefore, seems to be less significant. These different responses against GC may be due to cellular contexts. This mechanism is required for future analysis.

As documented here, CaD plays an important role in synaptic plasticity as well, because CaD is required for synaptic remodeling accompanied with chemically induced LTP. CaD plays also a role as a crucial downstream target in the stress/GC-induced effects on dendritic spine development. The abnormality of spine structure is considered to be associated with pathological dysfunction of the synapse. Indeed, psychiatric and neurologic disorders such as depression, schizophrenia, and Alzheimer's disease are characterized by pathologically altered spines (van Spronsen and Hoogenraad, 2010; Penzes et al., 2011). Thus, CaD may be involved in the stress-induced psychiatric disorders. Since spines and dendrites in young or aged rat brains are reported to exhibit different responsiveness against chronic stress (Dumitriu et al., 2010; Bloss et al., 2011), future study is required for this mechanism involving CaD. Our present study provides new insight into the molecular basis of stress/GC-induced synaptic remodeling, and detailed investigation of the relationship between stress/GCs and CaD should improve our understanding of stress-induced neuronal plasticity and the related psychiatric disorders.

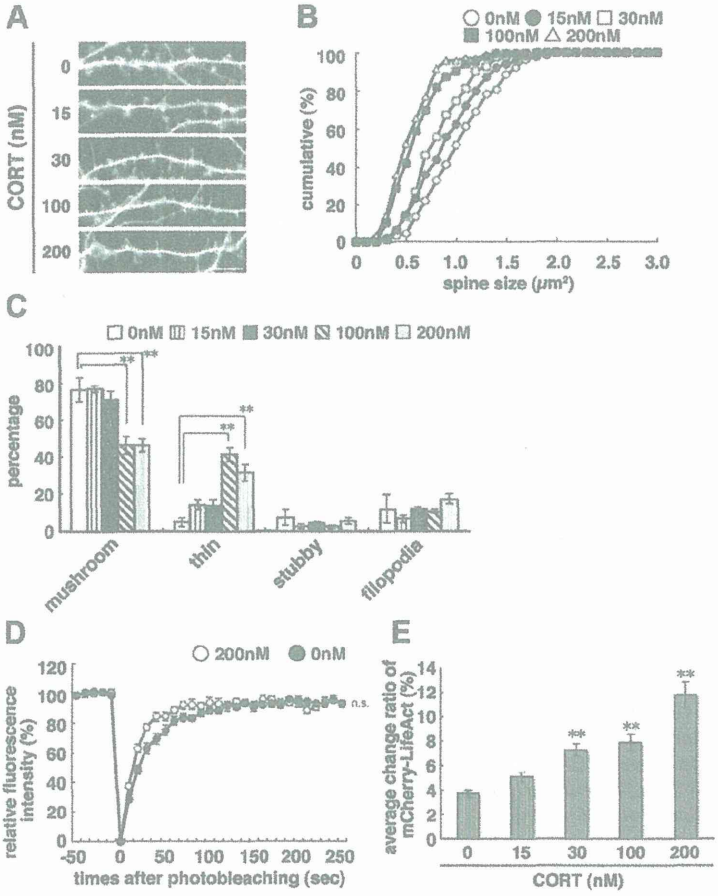

Figure 7. CORT effects on spine morphology and dynamics. *A*, Spine morphology in GFP-transfected hippocampal neurons cultured with 0–200 nM CORT (scale bar, 10 μm); (*B*) the graph shows spine sizes and their cumulative distributions. *C*, Dendritic protrusions, categorized by morphology: mushroom, thin, stubby, and filopodial. Data are means ± SE of values from at least 183 spines. *D*, The fluorescence recovery of mCherry-β-actin over time after photobleaching, measured in neurons cultured with 0 or 200 nM CORT. Data are means ± SE of values from 12 cells. *E*, CORT dose-dependent effects on spine F-actin dynamics were measured using mCherry-LifeAct. The graph shows the change rates of mCherry-LifeAct fluorescence intensity in spines. Data are means ± SE of values from at least 27 spines (**$p < 0.01$).

References

Becker JB, Monteggia LM, Perrot-Sinal TS, Romeo RD, Taylor JR, Yehuda R, Bale TL (2007) Stress and disease: is being female a predisposing factor? J Neurosci 27:11851–11855.

Bloss EB, Janssen WG, Ohm DT, Yuk FJ, Wadsworth S, Saardi KM, McEwen BS, Morrison JH (2011) Evidence for reduced experience-dependent dendritic spine plasticity in the aging prefrontal cortex. J Neurosci 31:7831–7839.

Dumitriu D, Hao J, Hara Y, Kaufmann J, Janssen WG, Lou W, Rapp PR, Morrison JH (2010) Selective changes in thin density and morphology in monkey prefrontal cortex correlate with aging-related cognitive impairment. J Neurosci 30:7507–7515.

Fischer M, Kaech S, Knutti D, Matus A (1998) Rapid actin-based plasticity in Dendritic spines. Neuron 20;847–854.

Fischer M, Kaech S, Wagner U, Brinkhaus H, Matus A (2000) Glutamate receptors regulate actin-based plasticity in dendritic spines. Nat Neurosci 3: 887–894.

Fukumoto K, Morita T, Mayanagi T, Tanokashira D, Yoshida T, Sakai A, Sobue K (2009) Detrimental effects of glucocorticoids on neuronal migration during brain development. Mol Psychiatry 14:1119–1131.

Gu J, Lee CW, Fan Y, Komlos D, Tang X, Sun C, Yu K, Hartzell HC, Chen G, Bamburg JR, Zheng JQ (2010) ADF/cofilin-mediated actin dynamics regulate AMPA receptor trafficking during synaptic plasticity. Nat Neurosci 13:1208–1215.

Hotulainen P, Hoogenraad CC (2010) Actin in dendritic spines: connecting dynamics to function. J Cell Biol 189:619–629.

Jiang M, Chen G (2006) High Ca^{2+}-phosphate transfection efficiency in low-density neuronal cultures. Nat Protoc 1:695–700.

Korkotian E, Segal M (2001) Regulation of dendritic spine motility in cultured hippocampal neurons. J Neurosci 21:6115–6124.

Lisman J (2003) Actin's actions in LTP-induced synapse growth. Neuron 38:361–362.

Liston C, Gan WB (2011) Glucocorticoids are critical regulators of dendritic spine development and plasticity in vivo. Proc Natl Acad Sci U S A 108:16074–16079.

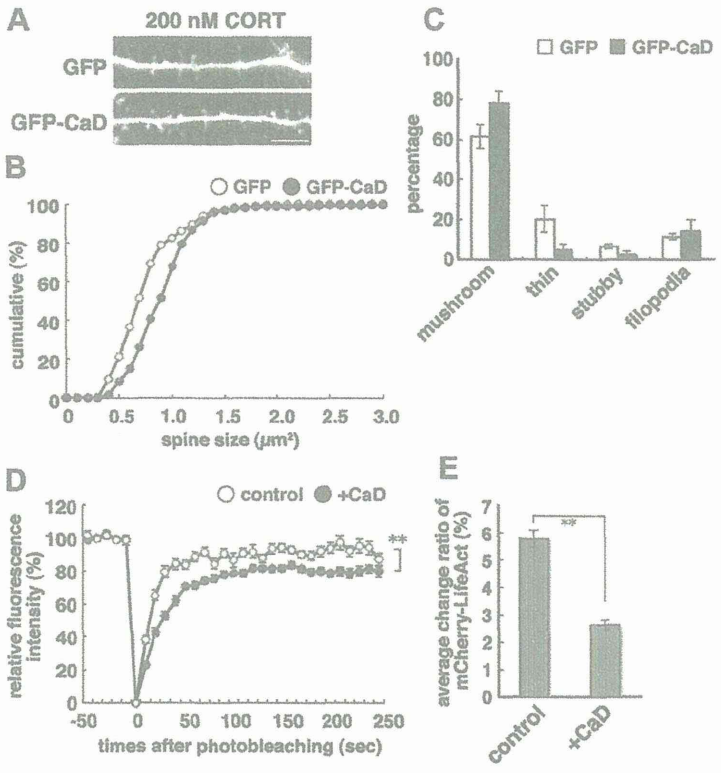

Figure 8. CaD recovers the CORT-induced dendritic spine changes. *A*, Spine morphology in neurons cultured with 200 nM CORT and transfected with GFP or GFP-CaD (scale bar, 10 μm); (*B*) the graph shows spine sizes and their cumulative distributions. *C*, Dendritic protrusions, classified by morphology: mushroom, thin, stubby, and filopodial. Data are means ± SE of values from at least 1214 spines. *D*, The fluorescence recovery of mCherry-β-actin over time after photobleaching, measured in neurons cultured with 200 nM CORT and transfected with a mock vector (control) or myc-tagged-CaD. Data are means ± SE of values from 16 cells (**$p < 0.01$). *E*, Spine F-actin dynamics in neurons cultured with 200 nM CORT and transfected by mock vector (control) or myc-tagged-CaD were measured using mCherry-LifeAct. The graph shows the change rates of mCherry-LifeAct fluorescence intensity in spines. Data are means ± SE of values from at least 21 spines (**$p < 0.01$).

Magariños AM, McEwen BS, Flügge G, Fuchs E (1996) Chronic psychosocial stress causes apical dendritic atrophy of hippocampal CA3 pyramidal neurons in subordinate tree shrews. J Neurosci 16:3534–3540.

Mayanagi T, Sobue K (2011) Diversification of caldesmon-linked actin cytoskeleton in cell motility. Cell Adh Migr 5:150–159.

Mayanagi T, Morita T, Hayashi K, Fukumoto K, Sobue K (2008) Glucocorticoid receptor-mediated expression of caldesmon regulates cell migration via the reorganization of the actin cytoskeleton. J Biol Chem 283:31183–31196.

McEwen BS (1999) Stress and hippocampal plasticity. Annu Rev Neurosci 22:105–122.

McEwen BS (2005) Glucocorticoids, depression, and mood disorders: structural remodeling in the brain. Metabolism 54:20–23.

McEwen BS (2010) Stress, sex, and neural adaptation to a changing environment: mechanisms of neuronal remodeling. Ann N Y Acad Sci 1204:E38–E59.

Modi N, Lewis H, Al-Naqeeb N, Ajayi-Obe M, Doré CJ, Rutherford M (2001) The effects of repeated antenatal glucocorticoid therapy on the developing brain. Pediatr Res 50:581–585.

Morita T, Mayanagi T, Sobue K (2012) Caldesmon regulates axon extension through interaction with Myosin II. J Biol Chem 287:3349–3356.

Otmakhov N, Khibnik L, Otmakhova N, Carpenter S, Riahi S, Asrican B, Lisman J (2004) Forskolin-induced LTP in the CA1 hippocampal region is NMDA receptor dependent. J Neurophysiol 91:1955–1962.

Penzes P, Cahill ME, Jones KA, VanLeeuwen JE, Woolfrey KM (2011) Dendritic spine pathology in neuropsychiatric disorders. Nat Neurosci 14:285–293.

Phillips NK, Hammen CL, Brennan PA, Najman JM, Bor W (2005) Early adversity and the prospective prediction of depressive and anxiety disorders in adolescents. J Abnorm Child Psychol 33:13–24.

Radley JJ, Sisti HM, Hao J, Rocher AB, McCall T, Hof PR, McEwen BS, Morrison JH (2004) Chronic behavioral stress induces apical dendritic reorganization in pyramidal neurons of the medial prefrontal cortex. Neuroscience 125:1–6.

Radley JJ, Rocher AB, Miller M, Janssen WG, Liston C, Hof PR, McEwen BS, Morrison JH (2006) Repeated stress induces dendritic spine loss in the rat medial prefrontal cortex. Cereb Cortex 16:313–320.

Sarmiere PD, Bamburg JR (2004) Regulation of the neuronal actin cytoskeleton by ADF/cofilin. J Neurobiol 58:103–117.

Sobue K, Sellers JR (1991) Caldesmon, a novel regulatory protein in smooth muscle and nonmuscle actomyosin systems. J Biol Chem 266:12115–12118.

Star EN, Kwiatkowski DJ, Murthy VN (2002) Rapid turnover of actin in dendritic spines and its regulation by activity. Nat Neurosci 5:239–246.

van Spronsen M, Hoogenraad CC (2010) Synapse pathology in psychiatric and neurologic disease. Curr Neurol Neurosci Rep 10:207–214.

von Bohlen Und Halbach O (2009) Structure and function of dendritic spines within the hippocampus. Ann Anat 191:518–531.

Watanabe Y, Gould E, McEwen BS (1992) Stress induces atrophy of apical dendrites of hippocampal CA3 pyramidal neurons. Brain Res 588:341–345.

Weinstock M (2008) The long-term behavioural consequences of prenatal stress. Neurosci Biobehav Rev 32:1073–1086.

Wellman CL (2001) Dendritic reorganization in pyramidal neurons in medial prefrontal cortex after chronic corticosterone administration. J Neurobiol 49:245–253.

Yano H, Hayashi K, Haruna M, Sobue K (1994) Identification of two distinct promoters in the chicken caldesmon gene. Biochem Biophys Res Commun 201:618–626.

Yemelyanov A, Czwornog J, Chebotaev D, Karseladze A, Kulevitch E, Yang X, Budunova I (2007) Tumor suppressor activity of glucocorticoid receptor in the prostate. Oncogene 26:1885–1896.

Original Paper

Cerebrovascular Diseases

Cerebrovasc Dis 2012;34:358–367
DOI: 10.1159/000343505

Received: May 16, 2012
Accepted: September 14, 2012
Published online: November 14, 2012

Postoperative Cerebral White Matter Damage Associated with Cerebral Hyperperfusion and Cognitive Impairment after Carotid Endarterectomy: A Diffusion Tensor Magnetic Resonance Imaging Study

Takamasa Nanba[a, b] Kuniaki Ogasawara[b] Hideaki Nishimoto[a]
Shunrou Fujiwara[a] Hiroki Kuroda[c] Makoto Sasaki[a] Kohsuke Kudo[a]
Taro Suzuki[c] Masakazu Kobayashi[b] Kenji Yoshida[b] Akira Ogawa[b]

[a] Advanced Research Center, [b] Department of Neurosurgery and [c] Cyclotron Research Center, School of Medicine, Iwate Medical University, Morioka, Japan

Key Words
Carotid endarterectomy · Cerebral white matter · Hyperperfusion · Cognition

Abstract
Background: Cerebral hyperperfusion after carotid endarterectomy (CEA), even when asymptomatic, often impairs cognitive function. However, conventional magnetic resonance (MR) imaging rarely demonstrates structural brain damage associated with postoperative cognitive impairment. MR diffusion tensor imaging (DTI) is potentially more sensitive for detection of white matter damage. Among the common parameters derived by DTI, fractional anisotropy (FA) is a marker of tract integrity, and mechanical disruption of axonal cylinders and loss of continuity of myelin sheaths may be responsible for reduced FA in white matter. The purpose of the present study was to determine whether postoperative cerebral white matter damage that can be detected by FA derived by DTI is associated with cerebral hyperperfusion after CEA and correlates with postoperative cognitive impairment. ***Methods:*** In 70 patients undergoing CEA for ipsilateral internal carotid artery stenosis (≥70%), cerebral blood flow (CBF) was measured using single-photon emission computed tomography (SPECT) before and immediately after CEA and on postoperative day 3. FA values in cerebral white matter were assessed using DTI before and 1 month after surgery. These values were normalized and analyzed using statistical parametric mapping 5. In each corresponding voxel in the pre- and postoperative normalized FA maps of each patient, a postoperative FA value minus a preoperative FA value was calculated, and a voxel with postoperatively reduced FA was defined based on data obtained from healthy volunteers. The number of voxels with postoperatively reduced FA was calculated and defined as the volume with postoperatively reduced FA. Neuropsychological testing, consisting of the Wechsler Adult Intelligence Scale Revised, the Wechsler Memory Scale and the Rey-Osterreith Complex Figure test, was also performed preoperatively and after the first postoperative month. Postoperative cognitive impairment on neuropsychological testing in each patient was defined based on data obtained from patients with asymptomatic unruptured cerebral aneurysms. ***Results:*** Post-CEA hyperperfusion on brain perfusion SPECT (CBF increase ≥100% compared with preoperative values) and postoperative cognitive impairment on neuropsychological testing were observed in 11 (16%) and 9 patients (13%), respectively. The volume with postoperatively reduced FA in

KARGER

Fax +41 61 306 12 34
E-Mail karger@karger.ch
www.karger.com

1015–9770/12/0346–0358$38.00/0

Accessible online at:
www.karger.com/ced

Kuniaki Ogasawara, MD
Department of Neurosurgery
Iwate Medical University
19-1 Uchimaru, Morioka 020-8505 (Japan)
E-Mail kuogasa@iwate-med.ac.jp

cerebral white matter ipsilateral to surgery was significantly greater in patients with post-CEA hyperperfusion than in those without ($p < 0.0001$). This volume in cerebral white matter ipsilateral to surgery was also significantly associated with postoperative cognitive impairment (95% confidence interval, 1.559–8.853; $p = 0.0085$). ***Conclusions:*** Cerebral hyperperfusion after CEA results in postoperative cerebral white matter damage that correlates with postoperative cognitive impairment.

Introduction

Cerebral hyperperfusion after carotid endarterectomy (CEA) is defined as a major increase in ipsilateral cerebral blood flow (CBF) after surgical repair of carotid stenosis that is well above the metabolic demands of the brain tissue [1, 2]. Cerebral hyperperfusion syndrome after CEA is characterized by unilateral headache, face and ocular pain, seizures, and focal symptoms related to cerebral edema or intracerebral hemorrhage [1–3]. Although the prognosis for patients with intracerebral hemorrhage is poor, the incidence is low (approx. 1%) [1–5]. Furthermore, neurological deficits in patients who develop cerebral hyperperfusion syndrome without experiencing subsequent intracranial hemorrhage tend to be reversible, as no major destruction of neural tissue due to intracranial hemorrhage occurs [5, 6]. By contrast, recent studies have demonstrated that the cerebral hyperperfusion phenomenon after CEA is often detected on CBF imaging and, even when asymptomatic, this phenomenon results in impairments of cognitive function [4, 6–8]. Such impairments may adversely affect quality of life [5, 8]. However, conventional magnetic resonance (MR) imaging, including diffusion-weighted imaging (DWI) and T2-weighted imaging, rarely demonstrates structural brain damage associated with postoperative cognitive impairment [7].

Another MR imaging technique, diffusion tensor imaging (DTI), is potentially more sensitive for detection of white matter damage [9]. DTI provides a quantitative, noninvasive method for delineating the anatomy of white matter pathways by measuring the magnitude and directionality of diffusion [10]. Among the common parameters derived by DTI, fractional anisotropy (FA) is a marker of tract integrity, and mechanical disruption of axonal cylinders and loss of continuity of myelin sheaths may be responsible for reduced FA in white matter [11]. FA shows stronger relationships with cognitive function than lesion volume displayed on conventional MR imaging in patients with age-related cognitive decline or cerebral small vessel disease [9, 12]. FA also correlates with cognitive function in chronic traumatic brain injury and Alzheimer's disease [13, 14].

The purpose of the present study was to determine whether postoperative cerebral white matter damage, which can be detected by FA derived by DTI, is associated with cerebral hyperperfusion after CEA and correlates with postoperative cognitive impairment.

Methods

Inclusion Criteria of Patients

Patients who were intended to undergo CEA and satisfied the following inclusion criteria were prospectively selected: age ≤75 years; ipsilateral cervical internal carotid artery (ICA) stenosis (≥70%); preoperative useful residual function (modified Rankin disability scale 0, 1 or 2); no ipsilateral carotid territory ischemic symptom before presentation to our department or ipsilateral carotid territory ischemic symptom that had occurred >2 weeks before presentation to our department; no massive cortical infarction confirmed by preoperative MR imaging using a 1.5-tesla imager (Signa MR/I; GE Healthcare, Milwaukee, Wisc., USA), including diffusion-weighted, T2-weighted and fluid-attenuated inversion recovery sequences, and obtaining written informed consent. Patients with new neurological deficits lasting for 2 weeks after surgery were excluded from the present study.

All study protocols were reviewed and approved by the institutional ethics committee.

CBF Measurements

CBF was assessed using [^{123}I]N-isopropyl-*p*-iodoamphetamine (IMP) and SPECT with a ring-type scanner (Headtome-SET 080; Shimadzu, Kyoto, Japan) before and immediately after CEA. In addition, patients with post-CEA hyperperfusion underwent a third CBF measurement in the same manner, 3 days after CEA. The IMP-SPECT study was performed as described previously [15], and CBF images were calculated according to the IMP autoradiography method [15, 16].

All SPECT images were transformed into standard brain size and shape by linear and nonlinear transformation using statistical parametric mapping (SPM) 99 software for anatomical standardization [17]. A 3-dimensional stereotaxic region-of-interest (ROI) template was used to automatically place 318 constant ROIs in both cerebral and cerebellar hemispheres [18]. ROIs were grouped into 10 segments (callosomarginal, pericallosal, precentral, central, parietal, angular, temporal, posterior, hippocampal and cerebellar) in each hemisphere according to the arterial supply. Eight (callosomarginal, pericallosal, precentral, central, parietal, angular, temporal, posterior) of these 10 segments were combined and defined as an ROI in the cortex of the cerebral hemisphere (fig. 1). Mean CBF was calculated in an ROI in the cerebral hemisphere ipsilateral to surgery before and after CEA. Post-CEA hyperperfusion was defined as a CBF increase of ≥100% (i.e. a doubling) compared with preoperative values, according to Piepgras et al. [1].

Intra- and Postoperative Management

All patients underwent surgery under general anesthesia. A continuous 8-channnel electroencephalography (EEG) tracing for detection of cerebral ischemia during ICA clamping was initiated after induction of anesthesia. No intraluminal shunt was used during ICA clamping in any patients. Mean duration of ICA clamping was 36 min (range, 28–48 min). In patients with post-CEA hyperperfusion, intensive control of arterial blood pressure between 100 and 140 mm Hg was instituted using intravenous administration of antihypertensive drugs immediately after SPECT. When CBF decreased and hyperperfusion resolved on postoperative day 3, pharmacological control of blood pressure was discontinued. However, when hyperperfusion persisted, systolic arterial blood pressure was maintained below 140 mm Hg. When hyperperfusion syndrome developed, the patient was placed in a propofol coma. A diagnosis of hyperperfusion syndrome required: (1) seizure, deterioration of level of consciousness, and/or development of focal neurological signs such as motor weakness, and (2) hyperperfusion on SPECT performed after CEA.

For detection of new intra- or postoperative lesions, all patients underwent T2-weighted and fluid-attenuated inversion recovery imaging and DWI using a 1.5-tesla whole-body imaging system within 7 days before and 1 day after surgery. Patients with cerebral hyperperfusion on CBF imaging performed immediately after surgery also underwent MR imaging on postoperative day 3 and after the first postoperative month. Furthermore, patients with cerebral hyperperfusion syndrome underwent additional MR imaging on the day on which symptoms developed. Two neuroradiologists (MS and KK) who were blinded to patient clinical information provided analysis of images and determined whether new lesions had developed postoperatively.

FA Measurements by DTI

DTI was performed using a 3.0-tesla superconductive MR imager with a gradient slew rate of 150 mT $m^{-1}ms^{-1}$ (Signa Excite HD; GE Healthcare) and an 8-channel head coil within 7 days before and 1 month after surgery. The following pulse sequences were used for DTI covering the entire brain: axial single-shot, spin-echo, echo-planar imaging (EPI); repetition time, 10,000 ms; echo time, 66 ms; 6 motion-probing gradient directions (b-value 1,000 s/m^2); matrix size, 128 × 128; field of view, 24 cm; slice thickness, 4.0 mm with 1.5-mm interslice gaps (voxel size, 1.9 × 1.9 × 4.0 mm); number of slices, 24; number of excitations, 3; parallel imaging reduction factor, 2, and acquisition time, 3 min 40 s.

For voxel-based analysis, we used SPM5 and original software developed with C/C++. SPM5 is freely available and distributed at the Wellcome Trust Centre for Neuroimaging web page (http://www.fil.ion.ucl.ac.uk/spm/), although this required MATLAB (The MathWorks, Natick, Mass., USA) as a software environment supplying numerous functions needed for image processing and statistical analysis in SPM5. For DTI voxel-based analysis, DTI parametric maps needed to be preprocessed using the techniques proposed in previous works [19, 20]. FA maps of each subject were masked using originally developed software with custom white matter masks, which were segmented using SPM5 from non-diffusion-weighted images (b = 0 s/mm^2). Using those masks, statistical analysis was performed only on voxels within the mask, and the effect of other tissues such as the gray matter and cerebrospinal fluid was decreased. As no templates of FA parametric maps were available in SPM5, the template was constructed from masked FA maps of 10 healthy subjects using the following method. First, the EPI template was used to normalize non-diffusion-weighted images and we applied the normalization parameter to the corresponding FA maps. Second, those normalized FA maps were smoothed with a 12-mm isotropic Gaussian kernel. Third, an averaged image of all smoothed FA maps of those subjects was defined as an FA template. Using the customized FA template, FA maps of each subject were again normalized. Finally, those normalized FA maps were smoothed with a 12-mm isotropic Gaussian kernel to improve the validity of statistical inferences and to reduce interindividual variation and coregistration errors.

In each corresponding voxel in the pre- and postoperative normalized FA maps of each patient, a postoperative FA value minus a preoperative FA value was calculated. As controls, 10 healthy volunteers (8 men; mean age, 33 years; range, 21–55 years) without any history of hypertension, diabetes mellitus, atrial fibrillation, pulmonary disease or presence of organic brain lesions, including

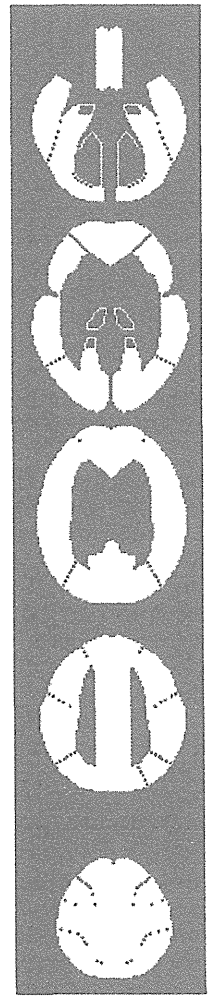

Fig. 1. Diagrams show the ROIs for a 3-dimensional stereotaxic ROI template for brain perfusion SPECT. White ROIs indicate the cerebral hemispheric cortex (callosomarginal, pericallosal, precentral, central, parietal, angular, temporal, posterior segments).

leukoaraiosis or asymptomatic lacunar infarction, on MR imaging underwent 2 separate DTI studies in the same manner. The interval between the two studies ranged from 1 month to 2 months. As a result, the mean – 2 SDs of the difference of the FA value (the second study value minus the first study value) was 0 to –0.05 in 26,664 voxels (24.9%), –0.05 to –0.10 in 60,683 voxels (56.6%), –0.10 to –0.15 in 17,425 voxels (16.2%), –0.15 to –0.20 in 2,381 voxels (2.2%) and –0.20 to –0.25 in 121 voxels (0.1%) from a total of 107,274 voxels in bilateral cerebral hemispheres. In each voxel in each patient, a difference of an FA value below the mean – 2 SDs of the value in the control group of healthy volunteers was defined as postoperatively reduced FA. In each cerebral hemisphere of each patient, the number of voxels with postoperatively reduced FA was calculated, and the ratio (%) of the number of voxels with postoperatively reduced FA to a total number of voxels of a unilateral cerebral hemisphere (53,637 voxels) was calculated and defined as the volume with postoperatively reduced FA.

Neuropsychological Evaluation

A battery of neuropsychological tests was administered, consisting of the Japanese translation of the Wechsler Adult Intelligence Scale Revised (WAIS-R) [21], the Japanese translation of the Wechsler Memory Scale [22], and the Rey-Osterreith Complex Figure test (Rey test) [23]. The WAIS-R provides measures of general intellectual function and generates a verbal and performance intelligence quotient (IQ). The Rey test evaluates copy and recall of a complex figure. As a result, 5 scores (WAIS-R verbal IQ; WAIS-R performance IQ; Wechsler Memory Scale; Rey copy and Rey recall) were used to evaluate cognitive function.

Neuropsychological tests were performed before and 1 month after surgery. All examinations were administered by a trained neuropsychologist who was blinded to the clinical information of patients.

As controls, 44 patients with asymptomatic unruptured cerebral aneurysms (17 men, 27 women; mean age, 56.8 years; range, 32–70 years) underwent the same neuropsychological tests before and 1 month after neck clipping by craniotomy [24]. None of the 44 patients had new postoperative neurological deficits or brain injury caused by surgery for aneurysms on postoperative computed tomography. Mean differences in each neuropsychological test score before and after neck clipping (postoperative scores – preoperative scores) were 2.4 ± 4.6 in WAIS-R verbal IQ, 4.8 ± 5.2 in WAIS-R performance IQ, 2.9 ± 8.1 in the Wechsler Memory Scale, 0.2 ± 1.1 in Rey copy, and 2.6 ± 4.2 in Rey recall. As a result, the mean difference – 2 SD was –6.8 for WAIS-R verbal IQ, –5.6 for WAIS-R performance IQ, –13.3 for Wechsler Memory Scale, –2.0 for Rey copy and –5.8 for Rey recall. For the neuropsychological test scores of each patient undergoing CEA, a deficit was defined as a postoperative test score < preoperative score minus the absolute value of the mean – 2 SDs of the difference between the 2 test scores in the controls. A patient was considered as having postoperative cognitive impairment when one or more postoperative neuropsychological scores showed a deficit.

Statistical Analysis

Data are expressed as means ± SD. The relationship between each variable and the volume with postoperatively reduced FA in the cerebral white matter ipsilateral to surgery was evaluated using the Mann-Whitney U test. The relationship between each variable and postoperative cognitive impairment was evaluated by univariate analysis using the Mann-Whitney U test or χ^2 test. Multivariate statistical analysis of factors related to postoperative cognitive impairment was also performed using a logistic regression model. Variables with $p < 0.2$ in univariate analyses were selected for analysis in the final model. Differences were deemed statistically significant for values of $p < 0.05$.

Results

Over a period of 22 months, 70 patients satisfied the inclusion criteria. None of the patients developed new neurological deficits that lasted for 2 weeks after surgery. Thus, all 70 patients were analyzed in the present study.

The mean (±SD) age of the patients (63 men, 7 women) was 67.9 ± 7.6 years (range, 44–82). Concomitant disease states and symptoms were recorded, including hypertension in 62 patients, diabetes mellitus in 27 patients and hyperlipidemia in 36 patients. Fifty patients evidenced ipsilateral carotid territory symptoms, including 28 patients with transient ischemic attack, 8 patients with transient ischemic attack and subsequent stroke, and 14 patients with stroke alone. Twenty patients showed asymptomatic ICA stenosis. Preoperative MR imaging demonstrated infarction in the hemisphere ipsilateral to the ICA stenosis in 43 patients and no infarction in 27 patients. The contralateral ICA was occluded in 5 patients, and 12 additional patients showed 60–95% stenosis in the contralateral ICA. According to categories graded by Arnold et al. [25], 6 (9%) and 1 (1%) patients exhibited moderate and severe EEG changes during ICA clamping, respectively. DWI using a 1.5-tesla imager performed 1 day after surgery showed new hyperintense lesions only in the cerebral hemisphere ipsilateral to CEA in 9 of the 70 patients (13%) when compared with preoperative DWI. The diameter of all new hyperintense lesions was <1.0 cm.

Post-CEA hyperperfusion on SPECT was observed in 11 patients (16%). In 9 of these 11 patients, hyperperfusion had resolved in the SPECT performed on postoperative day 3, and pharmacological control of blood pressure was discontinued. These patients did not eventually develop new neurological symptoms. The remaining 2 patients with post-CEA hyperperfusion experienced a progressive increase in CBF on postoperative day 3 and developed hyperperfusion syndrome. One of these patients experienced motor weakness of the upper and lower extremities on the side contralateral to surgery on postoperative day 4. Another patient experienced focal seizures as evidenced by motor disturbances of the upper extremity on the side contralateral to surgery 5 days after surgery. Propofol coma was induced in these 2 patients. Af-

Table 1. Analysis of factors related to volume with postoperatively reduced FA

Variables	Volume with postoperatively reduced FA (mean ± SD), %	p value
Age		0.8416
≥70 years (n = 35)	3.1 ± 4.6	
<70 years (n = 35)	2.3 ± 2.1	
Gender		0.8987
Male (n = 63)	2.8 ± 3.7	
Female (n = 7)	1.9 ± 1.1	
Hypertension		0.2717
Yes (n = 62)	2.9 ± 3.7	
No (n = 8)	1.5 ± 1.3	
Diabetes mellitus		0.8848
Yes (n = 27)	2.4 ± 2.3	
No (n = 43)	2.9 ± 4.2	
Hyperlipidemia		0.5254
Yes (n = 36)	2.6 ± 2.4	
No (n = 34)	2.8 ± 4.5	
Symptomatic lesion		0.9896
Yes (n = 50)	2.7 ± 3.9	
No (n = 20)	2.6 ± 2.7	
Infarction on preoperative MR imaging		0.6903
Yes (n = 43)	2.8 ± 4.2	
No (n = 27)	2.5 ± 2.3	
Bilateral lesions		0.9781
Yes (n = 17)	2.6 ± 4.0	
No (n = 53)	2.7 ± 3.5	
Duration of ICA clamping		0.6915
≥40 min (n = 19)	2.3 ± 1.9	
<40 min (n = 51)	2.9 ± 4.0	
EEG changes during ICA clamping		0.3370
Yes (n = 7)	5.0 ± 7.2	
No (n = 63)	2.5 ± 2.9	
New ischemic lesions on DWI on postoperative day 1		0.8126
Yes (n = 9)	3.6 ± 6.6	
No (n = 61)	2.6 ± 2.9	
Postoperative hyperperfusion		<0.0001
Yes (n = 11)	8.1 ± 6.0	
No (n = 59)	1.7 ± 1.5	

Table 2. Univariate analysis of factors related to postoperative cognitive impairment

Variables	Postoperative cognitive impairment		p value
	yes (n = 9)	no (n = 61)	
Age, years	67.0 ± 5.0	67.8 ± 7.9	0.4553
Male gender	9 (100)	54 (89)	0.5831
Hypertension	9 (100)	53 (87)	0.5841
Diabetes mellitus	4 (44)	23 (38)	0.7258
Hyperlipidemia	6 (67)	30 (49)	0.4791
Symptomatic lesion	6 (67)	44 (72)	0.7082
Infarction on preoperative MR imaging	6 (67)	37 (61)	>0.9999
Bilateral lesions	1 (11)	16 (26)	0.4376
Duration of ICA clamping, min	35.1 ± 6.6	37.0 ± 5.4	0.3121
EEG changes during ICA clamping	1 (11)	6 (10)	>0.9999
New ischemic lesions on DWI on postoperative day 1	1 (11)	8 (13)	>0.9999
Postoperative hyperperfusion	6 (67)	5 (8)	0.0002
Volume with postoperatively reduced FA, %	9.8 ± 5.7	1.6 ± 1.3	<0.0001

Values are means ± SD or numbers with percentages in parentheses.

ter termination of the propofol coma, these patients eventually experienced full recovery. None of the 11 patients with post-CEA hyperperfusion exhibited new lesions on MR imaging using a 1.5-tesla imager performed on postoperative day 3, the day on which symptoms developed, or after the first postoperative month.

Among the 70 patients studied, the volume with postoperatively reduced FA ranged from 0.1 to 21.0% (mean, 2.7 ± 3.6) in the cerebral hemisphere ipsilateral to surgery and from 0.1 to 5.4% (mean, 1.9 ± 1.4) in the contralateral cerebral hemisphere. Results of analysis of factors related to the volume with postoperatively reduced FA in the cerebral hemisphere ipsilateral to surgery are summarized in table 1. This volume was significantly greater in patients with post-CEA hyperperfusion than in patients without. No other variables were significantly associated with the volume showing postoperatively reduced FA.

At postoperative neuropsychological assessment, 9 patients (13%) showed postoperative cognitive impairment. Results of univariate analysis of factors related to postoperative cognitive impairment are summarized in table 2. The incidence of post-CEA hyperperfusion was significantly higher in patients with postoperative cognitive impairment than in those without. The volume with postoperatively reduced FA in the cerebral hemisphere ipsilateral to surgery was significantly greater in patients with postoperative cognitive impairment than in those without. Figure 2 shows relationships among volumes with postoperatively reduced FA in the cerebral hemisphere ipsilateral to surgery, post-CEA hyperperfusion and postoperative cognitive impairment. Other variables were not significantly associated with postoperative cognitive impairment. After eliminating variables that were closely re-

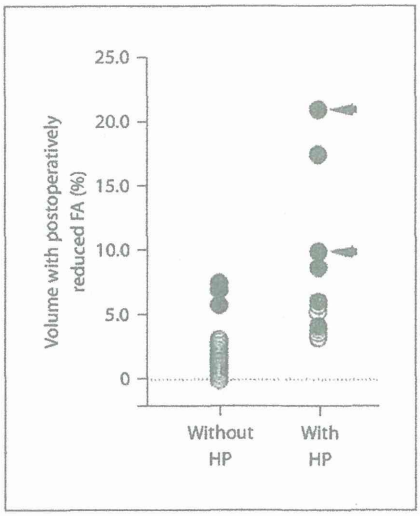

Fig. 2. Relationship between volume with postoperatively reduced FA in the cerebral white matter ipsilateral to surgery, postoperative hyperperfusion (HP) and postoperative cognitive impairment. The volume was significantly greater in patients with postoperative hyperperfusion than in those without ($p < 0.0001$) and was significantly greater in patients with postoperative cognitive impairment than in those without ($p < 0.0001$). Closed and open circles indicate patients with and without postoperative cognitive impairment, respectively. Arrows indicate patients with cerebral hyperperfusion syndrome.

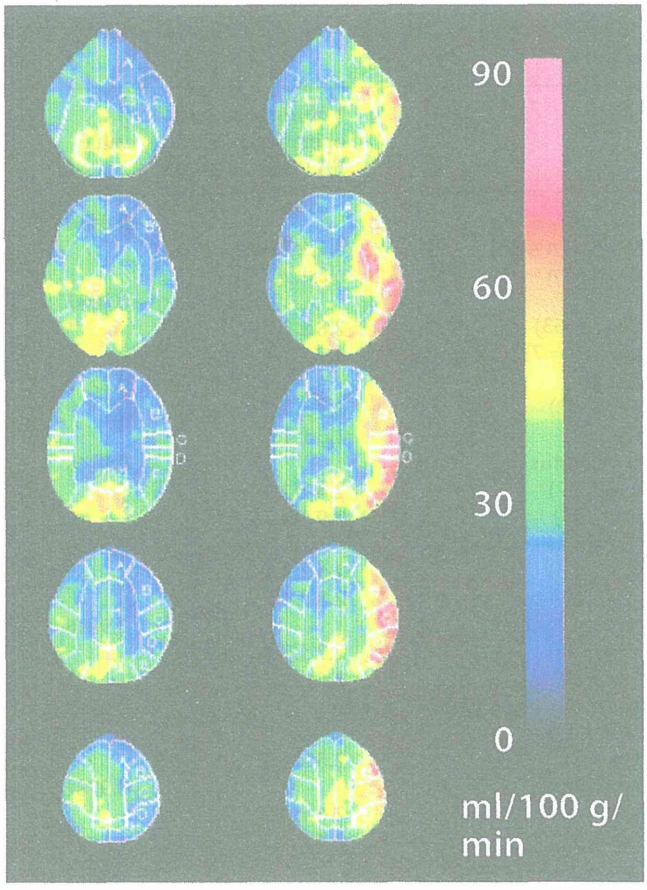

Fig. 3. A 73-year-old man with symptomatic left ICA stenosis (90%) exhibiting cerebral hyperperfusion syndrome and cognitive impairment after left CEA. Preoperative brain perfusion SPECT shows reduced blood flow in the left hemisphere (left row) where hyperperfusion develops immediately after surgery (right row).

lated to others, the following items with values of $p < 0.2$ in univariate analyses were adopted as confounders in the logistic regression model for multivariate analysis: post-CEA hyperperfusion; and volume with postoperatively reduced FA in the cerebral hemisphere ipsilateral to surgery. This analysis revealed that volume with postoperatively reduced FA in the cerebral hemisphere ipsilateral to surgery was significantly associated with postoperative cognitive impairment (95% confidence interval, 1.559–8.853; $p = 0.0085$). Figures 3 and 4 show SPECT and MR images, respectively, in a patient with cerebral hyperperfusion syndrome and cognitive impairment after surgery.

Discussion

Previous studies have demonstrated that patients with asymptomatic cerebral hyperperfusion on CBF imaging do not exhibit new postoperative lesions on conventional MR imaging and that even reversible vasogenic or cytotoxic edema on MR imaging develops in less than half of patients with cerebral hyperperfusion syndrome [7, 26]. This is consistent with results from the present study.

Post-CEA hyperperfusion often develops in the cerebral hemisphere ipsilateral to surgery, but not in the contralateral cerebral cortex [6]. The present study therefore evaluated the volume with postoperatively reduced FA only in the ipsilateral cerebral white matter. As a result, the volume was significantly greater in patients with post-CEA hyperperfusion than in those without. These data suggest that cerebral hyperperfusion after CEA results in postoperative white matter damage.

Postoperative white matter damage may also occur through other mechanisms. For example, a significant number of patients display evidence of gaseous or par-

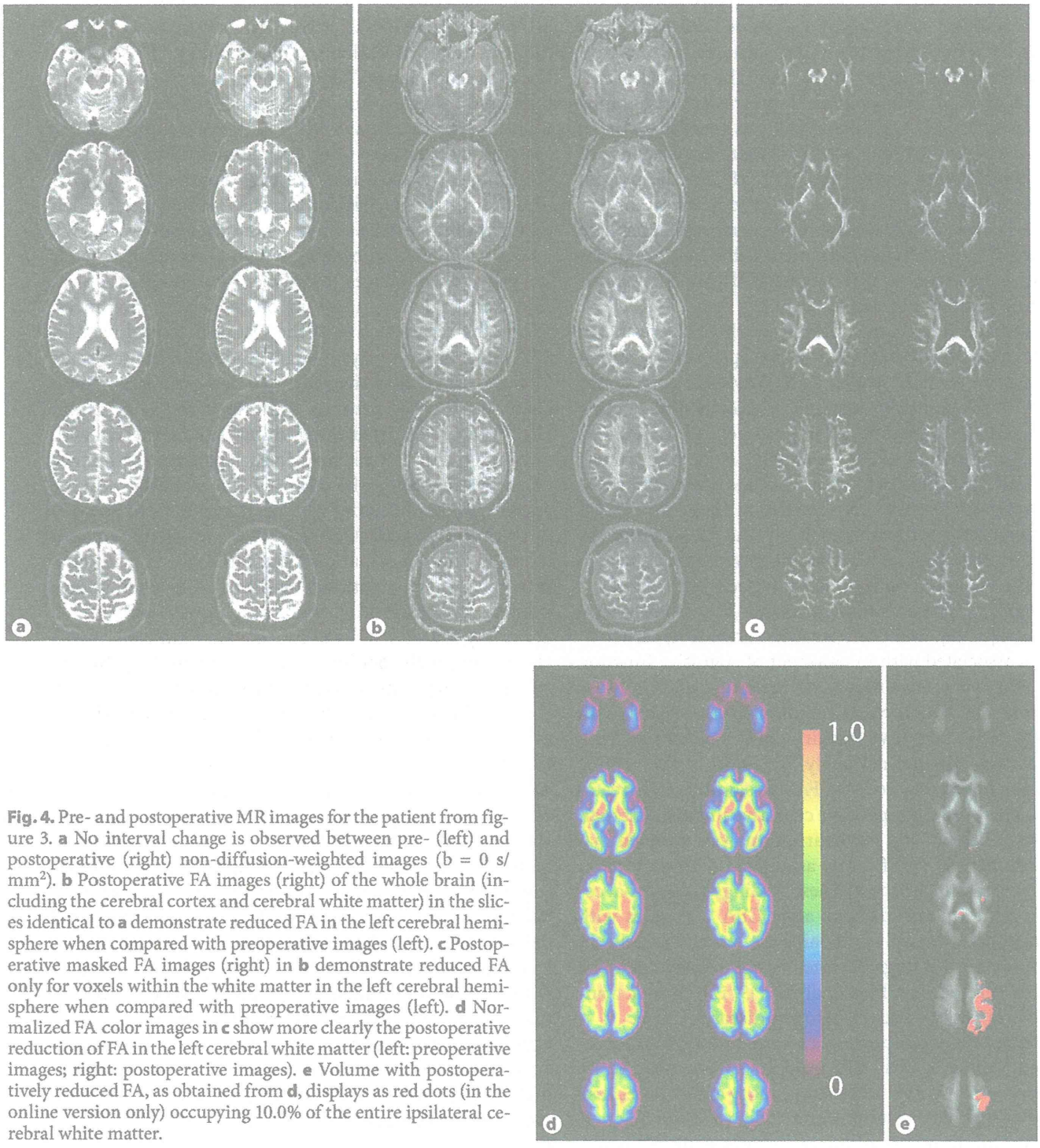

Fig. 4. Pre- and postoperative MR images for the patient from figure 3. **a** No interval change is observed between pre- (left) and postoperative (right) non-diffusion-weighted images (b = 0 s/mm^2). **b** Postoperative FA images (right) of the whole brain (including the cerebral cortex and cerebral white matter) in the slices identical to **a** demonstrate reduced FA in the left cerebral hemisphere when compared with preoperative images (left). **c** Postoperative masked FA images (right) in **b** demonstrate reduced FA only for voxels within the white matter in the left cerebral hemisphere when compared with preoperative images (left). **d** Normalized FA color images in **c** show more clearly the postoperative reduction of FA in the left cerebral white matter (left: preoperative images; right: postoperative images). **e** Volume with postoperatively reduced FA, as obtained from **d**, displays as red dots (in the online version only) occupying 10.0% of the entire ipsilateral cerebral white matter.

ticulate emboli in the middle cerebral artery during CEA [27]. In addition, new ischemic lesions on DWI performed within a few days after surgery are seen in approximately 10% of patients undergoing CEA, and the number of embolic signals on transcranial Doppler ultrasonography high-intensity transient signal analysis generated during CEA correlates strongly with postoperative evidence of new hyperintense lesions on DWI [28]. In the present study, although DWI performed 1 day after surgery showed new ischemic lesions in the cerebral hemisphere ipsilateral to CEA in 13% of patients, the presence or absence of the lesions was not associated with the volume showing postoperatively reduced FA.

Clamping of the carotid arteries during CEA results in a transient decrease in CBF in the ipsilateral cerebral hemisphere in many patients [2]. Any change in hemispheric CBF significant enough to damage the cerebral white matter may also result in postoperative reductions of FA. Intraoperative EEG monitoring is the most widely used and best documented method for the detection of hemispheric cerebral hypoperfusion due to carotid clamping [25]. In the present study, the EEG changes as well as the duration of ICA clamping were not associated with the volume showing postoperatively reduced FA.

Cognitive impairment occurs in 10–30% of patients after CEA [8, 29], and postoperative cerebral hyperperfusion is associated with impairment of cognitive function [5, 8]. However, conventional MR imaging does not always demonstrate structural brain damage associated with postoperative cognitive impairment [7], consistent with results from the present study. By contrast, the volume with postoperatively reduced FA was significantly greater in patients with postoperative cognitive impairment than in those without, and multivariate analysis revealed that the volume was significantly associated with postoperative cognitive impairment. These findings suggest that cerebral white matter damage after CEA correlates with postoperative cognitive impairment and is consistent with previous findings obtained in age-related cognitive decline, cerebral small vessel disease [9, 12], chronic traumatic brain injury and Alzheimer's disease [13, 14].

The present study possesses several limitations that require discussion. First, EPI used for DTI is affected by geometric distortions and susceptibility artifacts because of high sensitivity to inhomogeneity in the local magnetic field [30]. In addition, image distortion in EPI is observed more strongly at 3-tesla MR imaging than at 1.5-tesla MR imaging [31, 32]. In the present study, DTI acquisition was performed using an 8-channel phased-array head coil with parallel imaging technique to reduce image distortion [33, 34]. Second, the number of motion-probing gradient (MPG) directions used in the DTI technique was another limitation. We used only 6 MPG directions for acquiring DTI data, compared to the 12 or more axes used in recent studies [35, 36]. However, DTI techniques with more than 6 MPG directions require a relatively long acquisition time and cause motion artifacts in scanning for clinical use. We thus assume that 6 MPG directions may be efficient to assess white matter when using voxel analysis such as in the previous work [37]. Third, we applied smoothing with a Gaussian kernel for normalized FA images to reduce interindividual variation and registration errors on statistical inferences. While the different size of the Gaussian kernel used in DTI voxel-based analysis might lead to different results [38], the proportion of voxels with non-Gaussian residuals on the FA map plateaus when the kernel is $\geq$12 mm [20]. We therefore used a smoothing Gaussian kernel with 12 mm. Fourth, in each voxel in each patient, a difference of an FA value below the mean – 2 SDs of the value in the control group of healthy volunteers was defined as postoperatively reduced FA. In general, assuming that a population follows a normal distribution, a 95% confidential interval of the population is statistically included within its mean $\pm$ 2 SD. Postoperatively reduced FA was defined according to this statistical concept and numbers of voxels meeting such conditions were significantly greater in patients with postoperative cognitive impairment than in those without. Lastly, although neuropsychological tests are regarded as good measures of postoperative cognitive impairment [8, 29], criteria for defining significant impairment in neuropsychological tests can vary. Heyer et al. [29] assessed patients undergoing CEA and lumbar spine surgery using a battery of pre- and postoperative neuropsychological tests and defined patients undergoing spine surgery as a control group. Furthermore, they defined significant cognitive decline as performance that deteriorated below the absolute value of the mean – 2 SDs in the control group. The present study defined patients with asymptomatic unruptured cerebral aneurysms who underwent uneventful neck clipping by craniotomy as a control group. These subjects in the control group were approximately 10 years younger on average than patients undergoing CEA. Although all 5 neuropsychological test scores were postoperatively increased on average due to the 'practice effect' (an improvement in score when a patient is tested repeatedly) [8, 29], the definition of postoperative neuropsychological deficits in the present study may have under- or overestimated the true prevalence of deficits when compared with other studies.